A&A 487, 557–566 (2008)
DOI: 10.1051/0004-6361:200809505

Astronomy & Astrophysics

The initial luminosity and mass functions of the Galactic open clusters

A. E. Piskunov[1,2,3], N.V. Kharchenko[1,3,4], E. Schilbach[3], S. Röser[3], R.-D. Scholz[1], and H. Zinnecker[1]

[1] Astrophysikalisches Institut Potsdam, An der Sternwarte 16, 14482 Potsdam, Germany
e-mail: [apiskunov;nkharchenko;rdscholz;hzinnecker]@aip.de
[2] Institute of Astronomy of the Russian Acad. Sci., 48 Pyatnitskaya Str., 109017 Moscow, Russia
e-mail: piskunov@inasan.rssi.ru
[3] Astronomisches Rechen-Institut, Mönchhofstraße 12-14, 69120 Heidelberg, Germany
e-mail: apiskunov;nkhar;elena;roeser]@ari.uni-heidelberg.de
[4] Main Astronomical Observatory, 27 Academica Zabolotnogo Str., 03680 Kiev, Ukraine
e-mail: nkhar@mao.kiev.ua

Received 4 February 2008 / Accepted 25 April 2008

ABSTRACT

We aim at the construction of luminosity and mass functions for Galactic open clusters, based on integrated magnitudes and tidal masses. We also aim at studying the evolution of these functions, with the ultimate purpose of deriving the *initial* luminosity and mass distributions of star clusters, independent of model assumptions regarding the cluster mass-to-light ratio. Finally we aim at a new determination of the percentage of field stars that have originated in open clusters.

The integrated magnitudes are computed from individual photometry of cluster members selected from the ASCC-2.5 catalogue. The cluster masses we assumed to be the estimated tidal mass recently published by us elsewhere. Analysis of the cluster brightness distribution as a function of apparent integrated magnitudes shows that the cluster sample drawn from the ASCC-2.5 is complete down to apparent integrated magnitude $I_V = 8$, with 440 clusters and compact associations above this completeness limit. This, on average, corresponds to a completeness area in the solar neighbourhood with an effective radius of about 1 kpc.

The observed luminosity function can be constructed in a range of absolute integrated magnitudes $I_{M_V} = [-10, -0.5]$ mag, i.e. about 5 mag deeper than in the most nearby galaxies. It increases linearly from the brightest limit to a turnover at about $I_{M_V} \approx -2.5$. The slope of this linear portion is $a = 0.41 \pm 0.01$, which agrees perfectly with the slope deduced for star cluster observations in nearby galaxies. The masses of the Galactic clusters span a range from a few $M_\odot$ to $\log M_c/M_\odot \approx 5.5$. The mass function of these clusters can be fit as a linear function with log mass for $\log M_c/M_\odot > 2.5$, and shows a broad maximum between $\log M_c/M_\odot = 1.5$ and 2.5. For $\log M_c/M_\odot > 2.5$, the linear part of the upper cluster mass function has a slope $\alpha = 2.03 \pm 0.05$, again in agreement with data on extragalactic clusters. We regard this agreement as indirect evidence that the tidal masses for Galactic clusters and the luminosity-based masses for extragalactic clusters are on the same scale.

Considering the evolution of the cluster mass function now reveals a slight but significant steepening of the slope with increasing age from $\alpha = 1.66 \pm 0.14$ at $\log t \le 6.9$ to $\alpha = 2.13 \pm 0.08$ at $\log t \le 8.5$. This indicates that open clusters are formed with a flatter (initial) mass distribution than the overall observed cluster mass distribution averaged over all ages. Interestingly, the luminosity function of open clusters does not show the same systematic steepening with age as the mass function does.

We find that the initial mass function of open clusters (CIMF) has a two-segment structure with the slopes $\alpha = 1.66 \pm 0.14$ in the range $\log M_c/M_\odot = 3.37 \ldots 4.93$ and $\alpha = 0.82 \pm 0.14$ in the range $\log M_c/M_\odot = 1.7 \ldots 3.37$. The average mass of open clusters at birth is $4.5 \times 10^3\ M_\odot$, which should be compared to the average observed mass of about 700 $M_\odot$. The average cluster formation rate derived from the comparison of initial and observed mass functions is $\overline{\upsilon} = 0.4$ kpc^{-2} Myr^{-1}. Multiplying by the age of the Galactic disc ($T = 13$ Gyr) the predicted surface density of Galactic disc field stars originating from dissolved open clusters amounts to 22 $M_\odot$ pc^{-2} which is about 40% of the total surface density of the Galactic disc in the solar neighbourhood. Thus, we conclude that almost half of all field stars were born in open clusters, a much higher fraction than previously thought.

Key words. Galaxy: disk – Galaxy: open clusters and associations: general – solar neighborhood – Galaxy: stellar content – galaxies: star clusters

1. Introduction

Open clusters constitute an important part of a process transforming gas and dust into stars. They are observed as the most prominent parts in the regions of active star formation, or as tracers of the ceased star formation process in the general Galactic field. However, the role they are playing in this process has still not been fully understood. In spite of their prominence, there are indications that classical open clusters contribute only 10% or even less input (Wielen 1971; Miller & Scalo 1978; Piskunov et al. 2006) to the total stellar population of the Galactic disc. This contradiction can be explained either by an early decay of a considerable fraction of newly formed star clusters (see e.g. Tutukov 1978; Kroupa et al. 2001; Lamers et al. 2005) or by an insufficient knowledge of cluster formation statistics. In this context, one should note that the most important items of cluster formation like the distribution of cluster masses at birth (i.e., the initial mass function of star clusters) and the cluster formation rate are still poorly known.

Even in the close vicinity of the Sun, the only attempt to construct the luminosity function of open clusters (van den Bergh & Lafontaine 1984) is based on a sample of 142 clusters that, according to the authors, is to 2/3 complete within 400 pc. A mass function of Galactic open clusters is not yet available.

In contrast, extragalactic cluster populations have been actively investigated, especially during the present decade. The luminosity functions of remote clusters are determined both in active and regular galaxies (see e.g. Larsen 2002; de Grijs et al. 2003; Gieles et al. 2006, and references therein). For some galaxies, luminosity distributions of open clusters are converted to the mass functions via the assumed theoretical mass-luminosity relation (Zhang & Fall 1999).

Using extragalactic data for the study of cluster population gives certain advantages. When observing external galaxies, one is able to cover large areas of their surfaces and catch the brightest objects, which are intrinsically rare. This is rather difficult in the case of our own Galaxy since they could be hidden by a dusty environment. Also, different selection effects can be taken into account better in an external galaxy because its clusters are located at about the same distance from the Sun. Moreover, studies of extragalactic clusters give a key to our understanding of the cluster formation in different environments.

However, there are a number of problems related to studies based on extragalactic clusters. Samples of extragalactic clusters are restricted to relatively bright objects. There is a danger of a contamination of cluster samples by brightest stars and of losing sparse objects in the strong background. For example, Larsen (2002) finds that his sample in NGC 6949 is contaminated to about 20% by bright stars. The major problem is the necessity of transforming the observed luminosities into cluster masses. The corresponding transformations are mainly based on the luminosity of a dozen of the most massive stars, whereas cluster masses are defined by numerous stars of lower masses that are below the observing limit.

In our study of the local population of Galactic open clusters, we obtained data that now allow a reliable construction of their luminosity and mass functions. Our cluster sample contains 641 open clusters and 9 associations identified in the all-sky compiled catalogue ASCC-2.5 (Kharchenko 2001). For each cluster we determined a homogeneous set of cluster parameters including, among others, its distance, age, and tidal mass. The sample is found to be complete up to a distance of about 850 pc from the Sun (Piskunov et al. 2006). This completeness limit corresponds to a distance modulus ($V - M_V$) of about 10–10.5 (Schilbach et al. 2006) and allow probes of the luminosity function of open clusters that are much deeper than in other galaxies.

In this paper we aim at constructing the luminosity and mass functions of the Galactic open clusters and at comparing them to the data in other galaxies in order to touch the issue of universality of the cluster formation process in different environments. We also consider temporal variations of the two distributions. The ultimate purpose of this study is to construct the initial luminosity and mass distributions of star clusters independent of model assumptions on the M/L-ratio, to derive their parameters (the shape and limits), and to draw conclusions on the impact of these results on our understanding of the role of open clusters in the evolution of the stellar population of the Galactic disc.

The paper has the following structure. In Sect. 2 we briefly describe the input data and give the definitions used throughout the paper. Section 3 is devoted to the construction of cluster the luminosity and mass functions. In Sect. 4 we examine how cluster mass and luminosity functions evolve with time and build the cluster initial mass function. In Sects. 5 and 6 we discuss and summarise the results.

2. Data and definitions

In this paper we use the results of the previous work based on the study of 650 nearby open clusters identified in the ASCC-2.5. The sample includes 520 known objects and 130 open clusters detected within our project (Kharchenko et al. 2005b). For each star projected on a cluster area, a membership probability was determined in an iterative process that takes spatial, photometric, and proper motion distributions of stars into account within the corresponding area on the sky (Kharchenko et al. 2004). At the end of the iterations for each cluster, we obtained new coordinates of the cluster centre, the cluster size, the mean proper motion, the distance from the Sun, reddening, and age (Kharchenko et al. 2005a,b). These parameters were determined with data on the most probable members, i.e., stars having both kinematic and photometric membership probabilities higher than 61%. The results are included in the Catalogue of Open Cluster Data (COCD) and its Extension (Kharchenko et al. 2005a,b).

In Piskunov et al. (2007) we published masses of 236 clusters of our sample estimated from tidal radii determined with a three-parameter fit of King's profiles to the observed density distributions of cluster members. To obtain mass estimates for all clusters, we used these data to establish a relation between tidal radius and the observed semi-major axis of the apparent distribution of cluster members on the sky. The resulting tidal masses (i.e. calibrated tidal masses) for 650 clusters have been published in Piskunov et al. (2008). Though calibrated tidal masses of individual clusters are less accurate, their distribution fits well the distribution of the tidal masses based on the direct fitting of the King model. Moreover, because the parameters are homogeneous and more numerous, the calibrated masses are better suited to statistical investigations. In the following, we use the data on the calibrated tidal masses to study the luminosity and mass functions of the Galactic open clusters. Throughout the paper, masses are given in the units of solar masses.

Our list of 650 Galactic open clusters identified in the ASCC-2.5 includes 9 cluster-like associations (e.g. Vel OB2, Sco OB4), which require further commentary. These are objects, which are classified both as clusters and associations in the literature (e.g. α Per = Per OB3). They are included in our sample because their observed properties (spatial structure, internal kinematics, and stellar content) make them indistinguishable from regular open clusters, although they have larger sizes and higher masses. Hereafter we refer to them as cluster-like associations (see also Kharchenko et al. 2007).

We consider two young clusters, NGC 869 (also known as h Per) and NGC 884 (χ Per), as a single entity. They overlap in the projection on the sky, share a huge corona, and have a large number (more than 50%) of members in common, making an accurate determination of their individual tidal radii and masses rather difficult. Also, we exclude the cluster Mamajek 1 (η Chamaeleontis) for which we were able to identify only three members in the ASCC-2.5. According to Fig. 2, this cluster can be omitted without consequences for the results. Therefore, our final cluster sample includes 648 entities.

As a measure of cluster brightness needed for the construction of the luminosity function, we take the integrated magnitudes of the clusters. Doing so, we can directly compare our results with findings based on observations of open clusters in

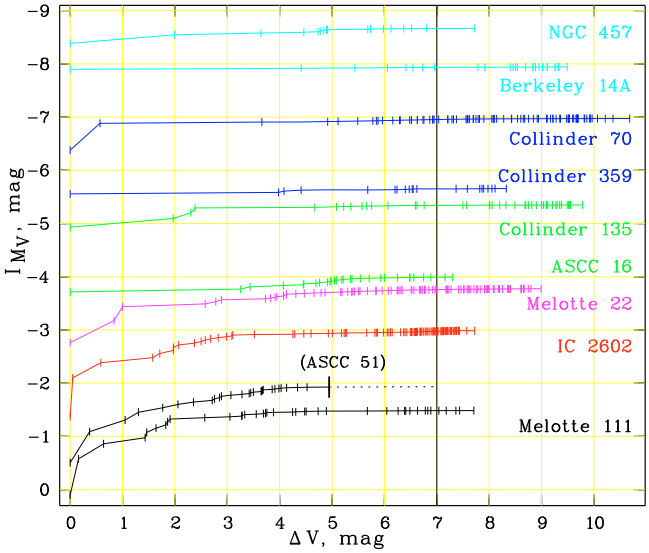

Fig. 1. Absolute integrated magnitude I_{M_V} profiles for 9 "template" clusters. ΔV is the magnitude difference between the brightest cluster star and fainter members. The vertical bars indicate individual stars. The contribution of stars fainter than $\Delta V = 7$ to I_{M_V} is small enough to be neglected. As an illustration of the reduction method applied to the observed integrated magnitudes of clusters, we show the profile of ASCC 51, which ends at $\Delta V \approx 5$ mag (longer vertical bar). The extension (dashed curve) to $\Delta V = 7$ mag is based on the template Mel 111, and it results in $\Delta I_V = 0.007$ mag.

other galaxies. We define apparent and absolute integrated magnitudes I_V and I_{M_V} as

$$I_V = -2.5 \log \left(\sum_i^{N_1} 10^{-0.4\, V_i} + 10^{-0.4\, \Delta I_V} \right),$$

and

$$I_{M_V} = I_V - (V - M_V),$$

where N_1 and V_i are the number and the apparent magnitudes of the most probable cluster members, respectively, and $(V - M_V)$ is the apparent distance modulus available in the COCD for each cluster. For "unseen" stars, ΔI_V is a magnitude correction, introduced to make the computed I_V and I_{M_V} independent of the range of stellar magnitudes actually observed in a given cluster.

To compute ΔI_V, we used $(I_{M_V}, \Delta V)$ profiles of nine "template" clusters shown in Fig. 1. The templates were selected to satisfy two constraints: to be uniformly distributed over the brightest stellar magnitudes of the clusters and to represent a sufficiently long observed main sequence (MS). In Fig. 1 we show the profiles as a function of $\Delta V_i = V_i - V_{\rm br}$ (V_i are individual magnitudes of the most probable members of a template and $V_{\rm br} = \min\{V_i\}$). At $\Delta V_i = 0$, the integrated magnitude I_{M_V} is identical to the absolute magnitude of the brightest cluster member. As one can see, stars that are seven or more magnitudes fainter than the brightest member ($\Delta V \geq 7$) do not have a significant impact on I_{M_V}. On the other hand, the typical absolute magnitude of cluster stars at $\Delta V = 7$ is brighter than $M_V = 6$ or $m > 0.9\, M_\odot$ in our sample. In this mass range, the mass functions of cluster stars are only weakly dependent on cluster age (Baumgardt & Makino 2003). This enables us to safely apply the above templates to the whole cluster sample.

A correction ΔI_V is computed for each cluster having a short MS as

$$\Delta I_V = I_V^{\rm fnt} - 2.5 \log \sum_{V_i = V_{\rm fnt}}^{V_{\rm br} + \Delta V} 10^{-0.4\, V_i}$$

after normalization of the suitable template profile (see Fig. 1). Here $V_{\rm br}$ and $V_{\rm fnt}$ are the brightest and faintest magnitudes of the most probable members in the cluster under consideration, V_i are template magnitudes, and $\Delta V = 7$ mag. The constant $I_V^{\rm fnt}$ is computed assuming that the cluster and the matching template have equal integrated magnitudes at $V_{\rm fnt}$. Since the integrated magnitude is mainly defined by the brightest cluster members, ΔI_V is relatively small: it is always less than 0.85 mag, with an average of 0.13 mag, and for 95% of the clusters $\Delta I_V < 0.3$. On the other hand, in 33 clusters the MS exceeds a length of 7 magnitudes. We truncated their profiles to $\Delta V = 7$, for homogeneity.

The other membership samples, i.e., samples including stars with a membership probability less than 61%, produce somewhat brighter magnitudes (on average, by about half a magnitude) but they are more strongly contaminated by field stars than is the sample of the most probable cluster members.

Throughout the paper we use the following definitions of cluster luminosity and mass functions. If the ΔN is the number of open clusters having absolute integrated magnitude in the range $[I_{M_V}, I_{M_V} + \Delta I_{M_V}]$ and which are observed in an area ΔS in the Galactic disc, then the luminosity function ϕ is

$$\phi(I_{M_V}) = \frac{1}{\Delta S} \frac{\Delta N}{\Delta I_{M_V}};$$

i.e., the luminosity function is a surface density distribution of open clusters over the integrated magnitude. Similarly, the mass function η is defined as a surface density distribution of open clusters over the logarithm of mass:

$$\eta(M_{\rm c}) = \frac{1}{\Delta S} \frac{\Delta N}{\Delta \log M_{\rm c}}.$$

Since the above distributions include clusters of all ages, it is reasonable to call $\phi(I_{M_V})$ and $\eta(M_{\rm c})$ the present-day luminosity and mass functions of clusters, or CPDLF and CPDMF, respectively. In the following, we also consider the luminosity and mass distributions of clusters confined by some upper limit of their age t. We call them current luminosity/mass functions of clusters or simply cluster luminosity/mass functions with the abbreviations CLF and CMF. To distinguish them from present-day distributions we denote them as $\phi_t(I_{M_V})$ and $\eta_t(M_{\rm c})$. Both functions are in fact cumulative with respect to age distributions.

The aim of the present paper is the construction of an initial mass function of star clusters, which indeed describes the initial distribution, i.e. the distribution after re-virialisation after residual gas expulsion (Kroupa & Boily 2002). Hereafter, we denote the initial luminosity/mass distributions as CILF and CIMF. A formal definition of these functions is given in Sect. 4.

Finally, we must keep in mind the evolutionary status of open clusters included in our sample. Since cluster membership is based on the proper motion data mainly obtained in the optical spectral range, we consider our sample as representative of optical clusters or "classical" open clusters. The embedded objects (e.g., the nearby cluster NGC 1333) are not included in our statistics since their members would be fainter than the limiting magnitude of $V \approx 11.5$ of the ASCC-2.5 if observed in the optical. Therefore, we assume the beginning of the transparency phase after the removal of the bulk of the placental matter to be

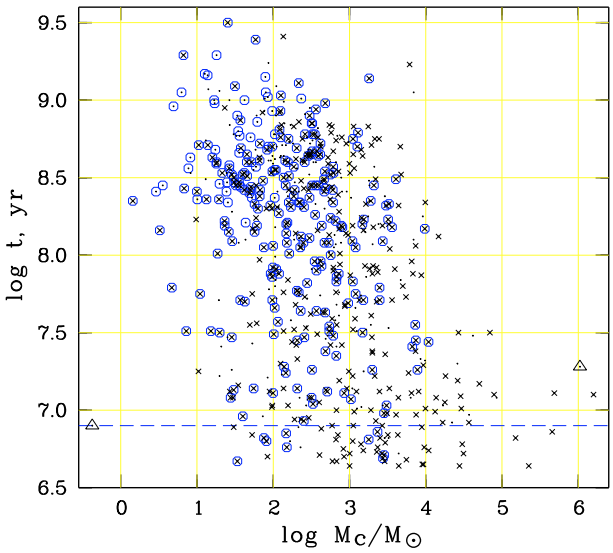

Fig. 2. Distribution of 650 clusters of our sample in ($\log t$, $\log M_c$)-diagram (dots). Open circles mark volume-limited sample of 257 clusters with a border of 850 pc. Crosses are 440 clusters from the magnitude-limited sample constructed in Sect. 3. Triangles mark two clusters omitted from the consideration (see Sect. 2). The dashed line shows the upper age limit of the youngest subsample discussed in Sect. 4.

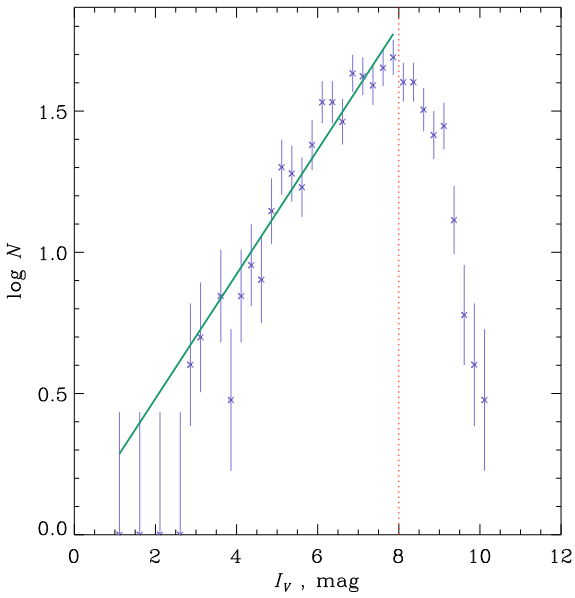

Fig. 3. Distribution of open clusters versus apparent integrated magnitude I_V computed from data on the most probable cluster members (crosses). The bars are corresponding Poisson errors, the solid line is a linear fit of the distribution and the vertical dotted line is the adopted completeness limit $\hat{I}_V$.

a starting point of the evolution of a classical open cluster. The corresponding age t_0 is defined by the lowest age of our clusters, that is, about 4 Myr.

3. Magnitude-limited sample of open clusters and the observed luminosity and mass functions

As shown in Piskunov et al. (2006), our sample can be considered as volume-limited with a boundary of about 850 pc. This volume contains 257[1] clusters, i.e. about one third of the total sample. However, the completeness distance varies if one considers clusters with different integrated magnitude. Very faint clusters can possibly be seen within slightly smaller distances. In contrast, very bright and massive clusters are seen at much greater distances but they are rare, and the limit of 850 pc is not sufficient for a realistic estimate of their average density. This presumption is supported by Fig. 2 where in an "age-mass" diagram we compare the distributions of all clusters with the clusters belonging to the volume-limited sample. For $\log t < 7.5$, the volume-limited sample does not represent the actual mass distribution of the young clusters and cannot be used for a realistic estimate of a mass function. The same is true for the distribution of integrated absolute magnitudes of young clusters. The problem can be solved if we could extract a cluster sample that is limited by a certain integrated magnitude. In this case, we can determine the completeness areas for clusters of different intrinsic brightnesses.

In Fig. 3 we show the distribution of our clusters in bins of apparent integrated magnitude I_V. Starting from $I_V \approx 3$, the logarithm of cluster numbers is linearly increasing with increasing I_V and reaches a maximum at $\hat{I}_V = 8$. We take $\hat{I}_V = 8$ as the completeness magnitude of our sample. In total, 440 clusters are brighter than $\hat{I}_V$. This increases the basis for the following statistical study by a factor of ≈1.7 (compared to the previous number of 257).

The cluster luminosity function ϕ is constructed as a function of integrated absolute magnitudes $I_{M_V,i}$ binned with a step size $\Delta I_{M_V} = 0.25$, as the sum of partial surface densities

$$\phi(I_{M_V,i}) = \frac{1}{\Delta I_{M_V}} \sum_j^{n_i} \frac{1}{\pi \hat{d}_j^2}.$$

Here $\hat{d}_j$ is the individual completeness distance corresponding to $\hat{I}_V = 8$, n_i is the number of clusters in the ith magnitude bin $I_{M_V,i}$, and $\sum n_i = 440$. Similarly, the mass function η is computed by using the logarithmic mass scale $\log M_{c,i}$ binned with a step size $\Delta \log M_c = 0.15$

$$\eta(M_{c,i}) = \frac{1}{\Delta \log M_c} \sum_j^{\nu_i} \frac{1}{\pi \hat{d}_j^2}$$

with ν_i the number of clusters in the mass bin $\log M_{c,i}$ and $\sum \nu_i = 440$. The completeness distance $\hat{d}_j$ for the jth cluster is given as

$$\log \hat{d}_j = 0.2\,[\hat{I}_V - I_{M_V,j} - 3.1\,E_j(B-V)] + 1,$$

where $E_j(B-V)$ is the reddening for the cluster.

In Fig. 4 we show the present-day luminosity function CPDLF constructed from 440 clusters. The CPDLF splits into a long quasi-linear portion at bright magnitudes, a turnover between $I_{M_V} = -3$ and -2, and an apparent decrease at fainter magnitudes. As expected, for Galactic star clusters the CPDLF can be observed as much deeper than for clusters in other galaxies. For the Large Magellanic Cloud (LMC), the faint limit is reached already at about $I_{M_V} = -5$, and it is much brighter in more distant galaxies (Larsen 2002).

Since the luminosity function is obtained from the distribution of clusters within the respective completeness limit, the

[1] This number does not include the two nearest open clusters UMa and the Hyades, for which we could not determine cluster membership via the standard pipeline and, therefore, were not able to obtain cluster masses and integrated magnitudes.

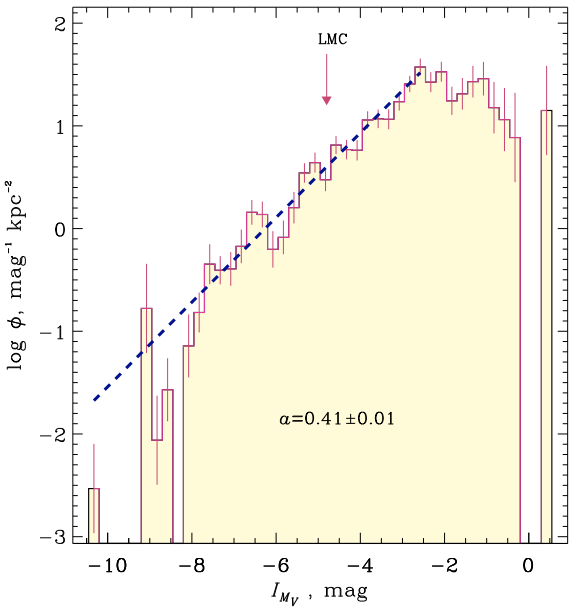

Fig. 4. Luminosity function of Galactic open clusters based on 440 local clusters brighter than the completeness limit $\hat{I}_V$ of the sample. The bars are Poisson errors, the dashed line shows a linear fit for the brighter part of the histogram ($I_{M_V} < -2.5$) where a is the corresponding slope. The arrow indicates the limit of integrated absolute magnitudes reached for open clusters in the LMC (see Larsen 2002).

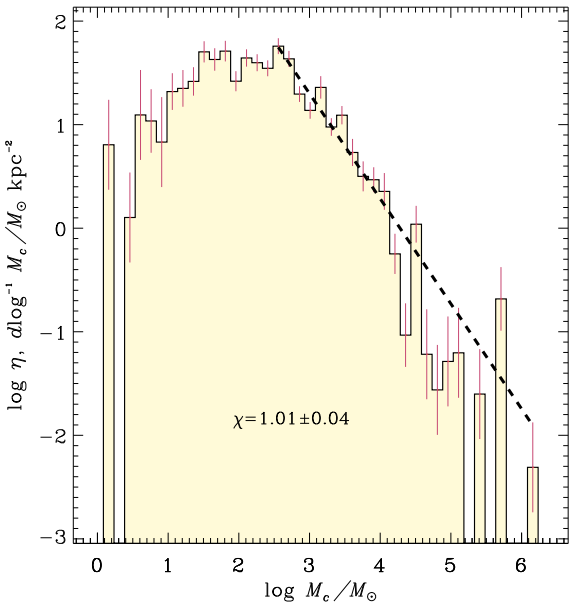

Fig. 5. Mass function of Galactic open clusters based on 440 local clusters brighter than the completeness limit $\hat{I}_V$ of the sample. The bars are Poisson errors, the dashed line shows a linear fit for the mass rich part of the histogram ($\log M_c > 2.5$) where χ is the corresponding slope.

turnover can be considered as a real feature of the CPDLF indicating a decrease of cluster density at $I_{M_V} > -2.5$. The slope a on the left side of the turnover ($I_{M_V} < -2.5$) is computed by fitting to the histogram (Fig. 4) a function

$$\log \phi = b + a\, I_{M_V},$$

where $a = 0.41 \pm 0.01$, $b = 2.58 \pm 0.07$. This corresponds to a slope of the cluster luminosity function $\alpha = 2.02 \pm 0.02$ counted in luminosity intervals (for a compatibility with stellar luminosity function we adopt that $\mathrm{d}N/\mathrm{d}L_V \propto L^{-\alpha}$). The slope α is frequently used for the description of the luminosity function of extragalactic clusters (see e.g. Larsen 2002) and can be expressed with the adopted definition as $\alpha = 2.5\, a + 1$.

The only attempt to obtain the luminosity function of Galactic open clusters was undertaken by van den Bergh & Lafontaine (1984). These authors constructed the CPDLF from integrated magnitudes computed by Sagar et al. (1983) for a sample of 142 clusters with accurate *UBV* photometry and proper motion membership. Their CPDLF was obtained for $I_{M_V} \le -2$ and with a slope $a = 0.2$ mag^{-1}, which is flat compared to our result. The authors regard the sample to be 2/3 complete within 400 pc and strongly incomplete outside this limit. However, no further details are given about the completeness issue (e.g. how it depends on cluster magnitude), and it is not possible to judge if their low value for the slope is a consequence of the incompleteness.

Larsen (2002) studied the luminosity functions of open clusters in six nearby spiral galaxies constructed from HST archive images, and in the LMC from literature data. Typically derived in the magnitude range $[-10, -7]$, the CPDLF slope varies within $a \approx 0.4 \ldots 0.6$ mag^{-1}. This result coincides with our finding for open clusters in the Milky Way. Further evidence for an agreement of the CPDLF slopes between Galactic and extragalactic clusters can be found e.g., in de Grijs et al. (2003).

The other interesting feature in our CPDLF is a deficiency of clusters for $I_{M_V} < -8$ compared to the fitted power law. A similar effect was observed by Larsen (2002) for extragalactic clusters.

The corresponding present-day mass function CPDMF of 440 clusters is shown in Fig. 5. We note similar details in the CPDMF that we have just observed for the CPDLF in Fig. 5. One recognises a quasi-linear portion in $\eta(M_c)$ for $\log M_c > 2.5$, a turnover at about $\log M_c = 2$, and a decrease for smaller masses. Again, we stress that the turnover of the CPDMF can be considered as a real feature, since the determination is based on unbiased cluster data. In the high-mass part of the histogram at $\log M_c > 2.5$, the CPDMF can be expressed in a canonical power-law form as

$$\log \eta = \log \eta^* - \chi \log M_c. \qquad (1)$$

A fit of Eq. (1) to the observed mass function provides $\chi = 1.01 \pm 0.04$ for the slope and $\log \eta^* = 4.3 \pm 0.14$ for the zero-point. A deficiency of clusters at the high-mass end ($\log M_c \gtrsim 4.0$) is less pronounced than we observe for the luminosity function, and discrepancies to the fitted relation are almost within Poisson errors.

Since all published data on mass functions of extragalactic clusters are based on the mass-luminosity relation used to convert the observed photometric or spectroscopic data into masses, only a formal comparison with our result is possible. In de Grijs et al. (2003), the slopes of the CPDMFs are listed for open clusters observed in four galaxies. Within a mass range $(10^3, 10^6\, M_\odot)$, a typical value of the CPDMF slope is $\alpha \approx 2$. On the logarithmic scale, this corresponds to $\chi \approx 1$ and agrees well with our results. We consider this result as indirect evidence of the coincidence of mass scales of Galactic and extragalactic clusters.

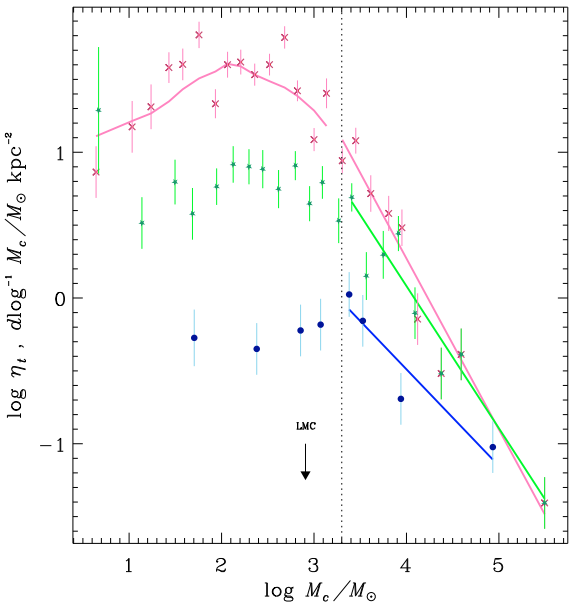

Fig. 6. Evolution of the mass function $\eta_t(\log M_c)$ of Galactic open clusters. Different symbols mark samples with different upper limits of cluster ages. The filled circles are for clusters with $\log t \le 6.9$, stars show CMF for $\log t \le 7.9$, and crosses indicate the CPDMF based on all 440 clusters ($\log t \le 9.5$). The bars are Poisson errors. The straight lines are the corresponding fits to linear parts of the mass functions at masses greater than $\log M_c = 3.3$ indicated by the vertical dotted line. The curve is the smoothed CPDMF at $\log M_c < 3.3$. The arrow indicates the lower mass limit reached for open clusters in the LMC.

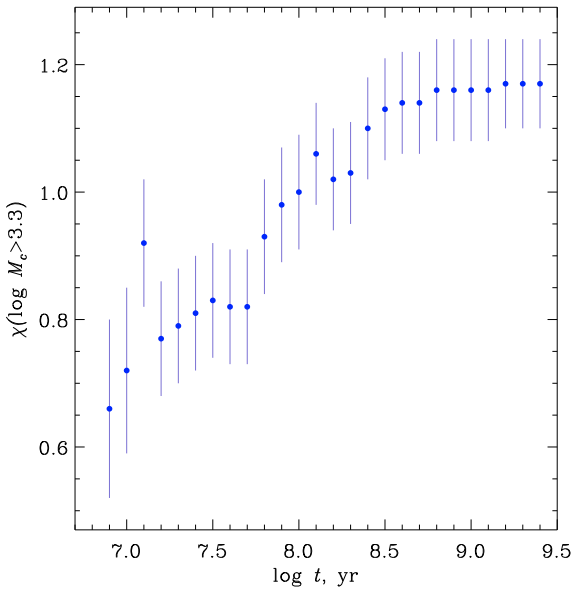

Fig. 7. Evolution of the slope χ of the mass function $\eta_t(\log M_c)$ at $\log M_c > 3.3$. The bars are Poisson errors.

4. Evolution of luminosity and mass functions; cluster IMF

Since star clusters evolve by changing the basic parameters (like mass and integrated luminosity), their mass and luminosity functions also undergo evolutionary changes. For stars, the impact of their evolution on the stellar mass and luminosity functions was revealed for the first time by Salpeter (1955), who developed a receipt for the construction of stellar initial luminosity/mass functions from present-day distributions.

Compared to stars, the case of stellar clusters is rather complicated. The evolution of a cluster follows two independent time scales. The first one is the nuclear time scale that governs the evolution of stars. The nuclear scale is primarily responsible for changing the cluster's luminosity and is related to the luminosity function of clusters. The second time scale is defined by the dynamical evolution and, especially, by two-body-relaxation-driven mass loss from clusters. Therefore, it is responsible for the evolution of the cluster mass function. Moreover, the nuclear lifetime does not depend on cluster mass, whereas the dynamical lifetime of a cluster is strongly related to its mass. These differences cause different schemes in the evolution of the luminosity and mass functions. Whereas the cluster luminosity function evolves in coordination with the evolution of the most massive cluster members, the mass function evolves faster at its low-mass end where the dynamical time is short.

Since the cluster luminosity function shows a more complicated evolution pattern, we start our consideration with the CMF.

4.1. Evolution of the mass function of star clusters

In Fig. 6 we show mass spectra of three cluster subsamples differing just by the upper limit of ages of the clusters. The first sample contains the 49 youngest clusters with ages less than $t_y \approx 8$ Myr ($\log t \le 6.9$). This is the lowest age limit where we have been able to construct a significant mass function. Hereafter, we call this subset the youngest sample. The second subsample includes additional moderately young clusters and contains 207 entities ($\log t \le 7.9$). Finally, we consider all 440 clusters ($\log t \le 9.5$). To improve the stability of the solutions, we made re-binning on the mass scale requiring at least five clusters per bin, but keeping the step of $\Delta \log M_c = 0.15$ whenever possible.

All three distributions demonstrate similar general patterns that can be separated into two parts. The more massive part at $\log M_c > \log M_c^* \approx 3.3$ is almost linear on the logarithmic scales $\log \eta_t$ and $\log M_c$ although the slope of the relation depends on the upper age limit. At lower masses, the CPDMF changes into a non-linear pattern. After reaching the maximum, the mass function of each sample starts to decrease. For the youngest sample, the low mass portion of the CMF is rather flat and the turnover is less significant. For older clusters, the CMF maximum is shifted to lower masses. Choosing other subsamples of clusters by varying the upper age limit from $\log t = 6.9$ to $\log t = 9.5$, we found that, at the age limit $\log t = 7.4$, the CMF reaches a maximum at $\log M_c \approx 2$. If we add older and older clusters, this location does not change anymore, although the value of the CMF-maximum increases.

On the abscissa of Fig. 6, we observe different mass ranges for the different subsamples. The lower mass limit depends significantly on the cluster age. The younger the clusters, the higher is the lower mass limit ($M_c^{\min} \approx 50\ M_\odot$ at $\log t \le 6.9$ and $M_c^{\min} \simeq 5\ M_\odot$ at $\log t \le 9.5$). We consider this as a manifestation of mass loss driven by the evolution of star clusters. On the other hand, the position of the bin of the highest masses seems to be independent of the sample considered. It varies from sample to sample only randomly, simply due to low number statistics of high-mass clusters.

In Fig. 7 we show the evolution of the slope of the linear portion of the CMF. Again, one can split its evolutionary path into two parts. The younger clusters show a steadily increasing slope from $\chi \approx 0.65$ at the upper limit $t \approx 8$ Myr to $\chi \approx 1.15$

Table 1. Parameters of the CMF for the youngest sample.

Fit	Segment	$\log M_c$ range	χ	$\log \eta^*$
S	low mass	$1.70 \ldots 3.30^1$	-0.18 ± 0.14	-0.69 ± 0.38
	high mass	$3.30^1 \ldots 4.90$	0.66 ± 0.14	2.16 ± 0.56
C	low mass	$1.70 \ldots 3.37^2$	-0.18 ± 0.14	-0.07 ± 0.60
	high mass	$3.37^2 \ldots 4.93$	0.66 ± 0.14	

[1] $\log M_c^* = 3.30$.
[2] $\log M_c^*$ from the solution of the continuity equation.

at $t \approx 600$ Myr. At older ages, the CMF slope practically does not change.

The mass functions η_t in Fig. 6 and their slopes χ in Fig. 7 describe cumulative mass distributions observed for clusters younger than t. Therefore, an increase in χ with increasing t is a consequence of adding older clusters, the mass spectra of which are similar or slightly flatter than the CIMF. At the limit, the slope of η_t corresponds to the slope of the CPDMF representing a mixture of clusters of different ages.

4.2. Initial mass function of star clusters

In the youngest sample, even the least massive clusters seem to have not had enough time to evolve dynamically. Therefore, we assume in the following that the youngest sample gives a good approximation of the CIMF, and the youngest point of the evolution curve in Fig. 7 is close to the slope of the CIMF. According to Fig. 6, we assume that Galactic clusters do form in a mass range from $M_c^{\min} = 50\,M_\odot$ to $M_c^{\max} = 3 \times 10^5\,M_\odot$.

The two segments of their CMF ($\log M_c < \log M_c^* \approx 3.3$, and $\log M_c > \log M_c^*$) can be scaled by a power law function with Eq. (1). The corresponding parameters are given in Table 1 (Fit S) where the fits are carried out separately for each of the two CMF segments. Again, since the CMF is based on clusters within the completeness limit, we consider the flattening $\eta_t(M_c)$ at $\log M_c < 3.3$ to be a real feature and not a signature of incompleteness.

To convert Eq. (1) in a convenient form suitable for the complete range of cluster masses, we adjust the solutions making use of the CMF continuity condition, so the mass M_c^* can be determined where for both segments $\eta_t(M_c^*) = \eta^*$. The results of these fits are given in Table 1 (Fit C). Obviously, the transformations do not affect the CMF slopes χ. Applying these definitions, we obtain

$$\eta_t = \frac{\mathrm{d}N}{\mathrm{d}\log M_c} = \eta^* \left(\frac{M_c}{M_c^*}\right)^{-\chi}. \tag{2}$$

For the construction of the CIMF we introduce a birth function $\beta(M_c, t)$ of star clusters as

$$\frac{\partial^2 N}{\partial M_c \partial t} = \beta(M_c, t).$$

Provided that the mass distribution of clusters at birth (CIMF) does not depend on time, we can factorize to get

$$\beta(M_c, t) = \zeta(M_c)\,\upsilon(t),$$

where $\zeta(M_c)$ is the CIMF, and $\upsilon(t)$ is the cluster formation rate (CFR). Provided that at $t > t_0$ the violent events related to infant mortality (see e.g. Kroupa et al. 2001) have generally ceased and a cluster starts its post-natal life, one can assume that within a short time interval following this moment, i.e. between $t_0 = 4$ Myr and $t_y = 8$ Myr, the mass loss from a cluster due to two-body relaxation seems to be insignificant (Lamers et al. 2005), and the relation between CMF and CIMF is straightforward:

$$\zeta(M_c) = \frac{\log e}{\overline{\upsilon}(t)\Delta t}\,\frac{\eta_t}{M_c},$$

where $\overline{\upsilon}(t)$ is the average cluster formation rate during the time Δt. Using Eq. (2) and the normalization condition

$$\int_{M_c^{\min}}^{M_c^{\max}} \zeta(M_c)\,\mathrm{d}M_c = 1,$$

we derive

$$\zeta(M_c) = \frac{k}{M_c^*}\left(\frac{M_c}{M_c^*}\right)^{-\alpha}, \tag{3}$$

where $\alpha = 1 + \chi$, and

$$k = \frac{\log e\,\eta^*}{\overline{\upsilon}(t)\Delta t} \tag{4}$$

is the normalization factor. With the parameters from Table 1 one gets

$$\alpha = \begin{cases} 0.82 \pm 0.14, & \text{for} \quad M_c^{\min} < M_c < M_c^* \\ 1.66 \pm 0.14, & \text{for} \quad M_c^* < M_c < M_c^{\max}, \end{cases}$$

and $M_c^* = 2.3 \times 10^3\,M_\odot$. The corresponding normalization factor is $k = 0.24$.

The two-segment CIMF can be understood in terms of the infant mortality process. The more massive clusters being able to survive the infant mortality and to keep the memory of their parental conditions in the embedded phase show a power law distribution scaling with their natal distribution. This interpretation is supported by the results of Lada et al. (1991), who studied dense cores within the molecular cloud L 1630 and found that the mass distribution of dense cores can be fitted by a power low with an exponent of -1.6. The result is in remarkable agreement with $-\alpha = -1.66$ we obtained for the CIMF at $M_c > 2.3 \times 10^3\,M_\odot$.

The low-mass segment of the CIMF probably consists for the major part of remnants of clusters damaged during the infant mortality phase and therefore lost memory of their recent past. Their mass distribution in the logarithmic scale resembles rather white noise. On the other hand, among young low-mass clusters, there may be a fraction that already had low masses at birth. Although the number of remnants and originally low-mass clusters is relatively large, their proportion is considerably less than the one they had if they would follow the power law of the more massive clusters.

Using the conclusions of a recent study of the influence of the gas expulsion phase on the shape of the resulting CIMF (Parmentier et al. 2008), we infer that the empirical CIMF derived in the present paper is compatible with the scenario of a low, randomly distributed star formation efficiency with an average of 20% and a dispersion of 3%.

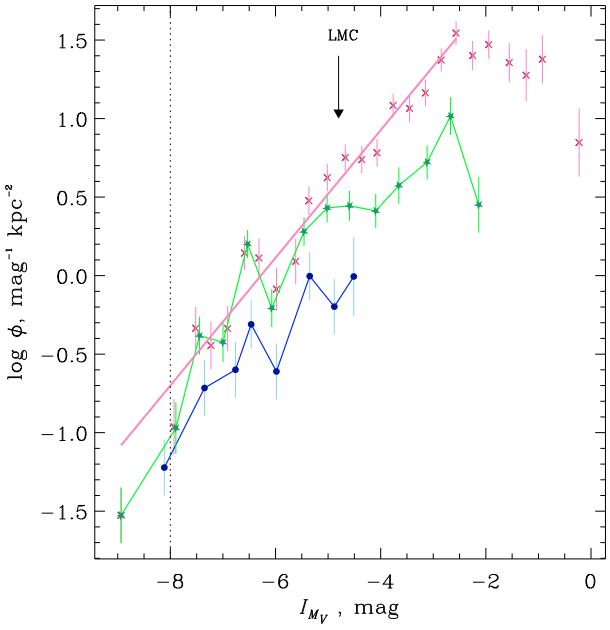

Fig. 8. Evolution of the luminosity function $\phi(I_{M_V})$ of Galactic open clusters. Different symbols mark samples with different upper limits of cluster age. The filled circles are for clusters with $\log t \le 6.9$, stars show CLF for $\log t \le 7.9$, and crosses indicate the CPDLF based on all 440 clusters ($\log t \le 9.5$). The bars are Poisson errors. The arrow indicates the observed limit of integrated absolute magnitudes reached for open clusters in the LMC. The dotted vertical line at $I_{M_V} = -8$ separates the luminous part where the CLF deficiency was observed for extragalactic clusters by Larsen (2002).

4.3. Evolution of luminosity function of star clusters

The evolution of the luminosity function of Galactic star clusters is shown in Fig. 8. Similar to the mass function, the CLF apparently includes two regimes (although less clearly distinguishable from each other than in the CMF case). The dominant feature is the linear regime of the CLF, occupying the bulk of brighter magnitudes up to $I_{M_V} \approx -2.5$, and a minor detail is a tail at fainter magnitudes. However, since the evolution of the luminosity function is governed mainly by stellar evolution, and only at the end of cluster life by dynamical effects, there is no direct correspondence between absolute magnitude and mass of clusters. In most of the CLF bins of absolute magnitude, we find a mixture of masses and evolutionary states. Only at the extremes of the magnitude scale, there are clusters of more or less "pure" evolutionary status. As a result, the initial luminosity function of open clusters can be taken from the distribution of the youngest clusters ($\log t \le 6.9$) at $I_{M_V} < -5.5$ where the clusters belong to the massive portion of the CIMF ($\log M_c > 3.3$), and the tail of the CPDLF at $I_{M_V} > -2$ consists mainly of decaying clusters with masses less than $\approx 100\, M_\odot$ i.e., after the CPDMF maximum.

Contrary to the CMF, the luminosity function at $-8.0 < I_{M_V} < -5.5$ does not show any evolution of the slope with time. It seems that, with increasing age, the CLF is just moving along the ordinate due to the arrival of newborn clusters without changing the shape and extends to fainter magnitudes due to the aging effect (fading of the brightest stars).

5. Discussion of the results

Based on this study on local Galactic clusters, we find that, in the immediate vicinity of the Sun, young ($\log t \le 6.9$) open clusters are present within a wide range of masses. The mass range extends from the highest masses – observed also in other galaxies – to a few tens of solar mass. This is a strong hint that the population in the solar neighbourhood is typical of spiral galaxies. In quite a natural way, cluster-like associations (see Sect. 2) form the high-mass end of the CPDMF; in other words, they represent the same population of the Galactic disc as young open clusters. A comparison of our luminosity and mass functions of star clusters with those in other galaxies, which we discussed in Sect. 3, strongly indicates a universal law of cluster formation, which is only weakly dependent on the environment. The issue of the universality of the cluster initial mass function in different galaxies is discussed in more detail by de Grijs et al. (2003).

Studying the CPDLF of extragalactic clusters, Larsen (2002) notes a depletion of the CPDLF at $I_{M_V} < -8$ in three galaxies. The author explains this effect by a possible increase in the steepness of the CPDLF. Gieles et al. (2006) confirm the existence of this precipitous drop in the cluster luminosity functions of the spiral galaxies NGC 6946 and M51 and explain this by assuming two-segment-, or Schechter CIMFs, in these galaxies. We observe the same feature in the luminosity function of Galactic clusters, too. Unfortunately, the ASCC-2.5 sample is restricted to the solar neighbourhood and does not include enough of the brightest clusters to be compared with the brightest limit of the extragalactic CPDLFs. As noted at the end of the last section, the parallel slope of the CPDLF for samples of different ages in the range $-8 \le I_{M_V} \le -5$ is a consequence of the continuity equation. A depletion at $I_{M_V} < -8$ suggests that no open clusters are born (or leave their parental cloud) with an absolute integrated magnitude much brighter than $I_{M_V} = -8$. A caveat is the poor statistics (only a few extragalactic clusters and no Galactic ones).

From the physical point of view, the observed deficiency might correspond to a gap caused by so-called "type II embedded clusters" (Kroupa & Boily 2002), which are massive enough to produce plenty of O stars providing fast gas expulsion and parent cluster decay. The low-mass limit of this cluster family should be in the vicinity of $\log M_c = 4.5$ in this case.

Lada & Lada (2003) have compiled a catalogue of about 100 embedded clusters within 2.4 kpc from the Sun. The sample contains some optical objects and is partly overlapping with our data. Using models of the luminosity function, Lada & Lada (2003) scaled the IR counts within the areas studied, estimated cluster masses, and constructed a mass function of embedded clusters. Typically, the clusters are distributed over a mass range from 50 to 1000 $M_\odot$ and thus, related the low-mass part of our CIMF. Based on "reasonably complete subsamples", the mass distribution function $M_c\, dN/d\log M_c$ increases approximately linear with M_c. This indicates that the CMF of embedded clusters $dN/d\log M_c$ is nearly constant and agrees with low-mass CIMF (see Table 1).

The newly determined CIMF and CPDMF have major implications for the evolution of the Galactic disc population. The average mass of forming clusters can be calculated from Eq. (3):

$$\overline{M}_c^{\rm CIMF} = \int_{M_c^{\rm min}}^{M_c^{\rm max}} M_c\, \zeta(M_c)\, dM_c.$$

With the parameters determined in Sect. 4.2, we find that $\overline{M}_c^{\rm CIMF} = 4.5 \times 10^3\, M_\odot$. The accuracy of this estimate depends on the accuracy of the CIMF parameters and, in particular, on the adopted integration limits. For example, by excluding the

highest mass bin (i.e., a shift of $M_c^{\max}$ from $3 \times 10^5\,M_\odot$ to to $10^4\,M_\odot$) from consideration, one obtains $\overline{M}_c^{\rm CIMF} = 1.4 \times 10^3\,M_\odot$.

The average mass of the presently observed clusters $\overline{M}_c^{\rm CPDMF}$ can be found from the CPDMF by its integration as

$$\overline{M}_c^{\rm CPDMF} = \frac{\int\limits_{\log M_c^{\min}}^{\log M_c^{\max}} M_c\,\eta(M_c)\,{\rm d}\log M_c}{\int\limits_{\log M_c^{\min}}^{\log M_c^{\max}} \eta(M_c)\,{\rm d}\log M_c}.$$

Taking the mass limits and the CPDMF from Fig. 6, we get $\overline{M}_c^{\rm CPDMF} \simeq 700\,M_\odot$. The accuracy of this value is estimated to be about 30%. The value of $\overline{M}_c^{\rm CPDMF}$ coincides perfectly with what is usually assumed for open clusters. The average age of the presently observed clusters computed in the same way is equal to about 260 Myr. We stress that this estimate is based on purely empirical grounds. A comparison of $\overline{M}_c^{\rm CIMF}$ and $\overline{M}_c^{\rm CPDMF}$ indicates that, during the first 260 Myr of its evolution, a typical open cluster loses about 60%–80% of its initial mass. We consider this as evidence of the importance of this phase in the evolution of open clusters. The average mass-loss rate based on these numbers then ranges from 3 to 14 $M_\odot\,{\rm Myr}^{-1}$. Since this estimate follows from observed masses of clusters, it includes both, mass loss due to stellar evolution and dynamical ejection of cluster stars.

The average surface density of open clusters in the solar neighbourhood n_c can be computed as

$$n_c = \int\limits_{\log M_c^{\min}}^{\log M_c^{\max}} \eta(M_c)\,{\rm d}\log M_c \approx 86\ {\rm kpc}^{-2}.$$

This is about 25% lower than was estimated in our study of the cluster population (Piskunov et al. 2006) on the basis of a volume-limited sample of local clusters closer than 850 pc. This disagreement can be explained by our omitting of clusters with $\hat{I}_V > 8$ in the present estimate. When taken into account, the estimates differ only by about 10%, which may result from the different methods of the sample extraction, i.e. the construction of volume-limited versus magnitude-limited samples.

Let us estimate the input of open clusters into the Galactic disc population and consider the total mass of optical star clusters that were formed during the history of the Galactic disc. The surface density of the Galactic disc stars having passed through an open cluster phase can be written as

$$\Sigma = \overline{\upsilon}\,T\,\overline{M}_c^{\rm CIMF},$$

where $T = 13$ Gyr is the age of the Galactic disc, and $\overline{\upsilon} = 0.4\ {\rm kpc}^{-2}\,{\rm Myr}^{-1}$ is the CFR determined via Eq. (4). This value is determined as an average over the past 4 Myr and has to be compared with other determinations. For optical clusters, we find similar results in the literature: e.g. $0.45\ {\rm kpc}^{-2}\,{\rm Myr}^{-1}$ in Battinelli & Capuzzo-Dolcetta (1991), and $0.25\ {\rm kpc}^{-2}\,{\rm Myr}^{-1}$ in Elmegreen & Clemens (1985). For embedded clusters, a much higher formation rate of $2{-}4\ {\rm kpc}^{-2}\,{\rm Myr}^{-1}$ is obtained by Lada & Lada (2003). This may be regarded as evidence of a considerable infant mortality among embedded clusters.

Assuming that the recent average CFR has not changed during the history of the Galactic disc one finds that for $\overline{M}_c^{\rm CIMF} = 4.5 \times 10^3\,M_\odot$

$$\Sigma = 22\,M_\odot\,{\rm pc}^{-2}.$$

This amount corresponds to about 40% of the total surface density of the Galactic disc in the solar neighbourhood that, according to Holmberg & Flynn (2004) is $56 \pm 6\,M_\odot\,{\rm pc}^{-2}$. From data on embedded clusters, Lada & Lada (2003) find $\Sigma = 10{-}30\,M_\odot\,{\rm pc}^{-2}$. The value of $\Sigma = 22\,M_\odot\,{\rm pc}^{-2}$ obtained here is considerably higher than the previous estimates for the input of open clusters to the observed stellar population of the Galactic disc that is quoted as about 10% (see Miller & Scalo 1978; Piskunov et al. 2006) or even less than 10% (Wielen 1971). These rather low estimates can be explained by several situations: they are based either on insufficient cluster statistics or on cluster masses from underestimated stellar counts, and on uncertain virial masses of open clusters or on arbitrarily chosen estimates of typical cluster contents. The newly derived value of Σ is in agreement with indirect evidence of binary population statistics (see Kroupa 1995). This value significantly readdresses the problem of the main sources of the Galactic disc population and indicates open clusters to be one of the major factories of field stars, in line with the fact that a major fraction of star formation seems to occur in embedded clusters (Zinnecker et al. 1993; Lada & Lada 2003; Megeath et al. 2005).

6. Summary and conclusions

Using the integrated magnitudes computed from individual photometry of cluster members available in the ASCC-2.5, we found that the sample of 648 clusters drawn from this catalogue is complete for apparent integrated magnitudes brighter than 8 mag, with 440 clusters above this completeness limit. The corresponding completeness distances depending on the brightness of clusters are typically between 1 and 3 kpc, although some prominent clusters can be seen up to distances of 10 kpc and more.

The CPDLF constructed on the basis of the complete sample is observed in the range of $I_{M_V} = [-10, -0.5]$ mag, i.e. about 5 mag deeper than observable in nearby galaxies. It increases from the brightest limit to a turnover at about $I_{M_V} \approx -2.5$ and slowly falls down towards fainter magnitudes. We consider the turnover to be a real feature reflecting the behaviour of Galactic open clusters. At magnitudes brighter than the turnover position, the CPDLF is linear with a slope $a = 0.41 \pm 0.01$ (or $\alpha = 2.02 \pm 0.02$), which is in perfect agreement with the observed slopes of cluster luminosity functions in nearby spiral galaxies, although these show a higher star formation activity.

The masses of Galactic open clusters cover a range from several tens to hundreds of thousands of solar masses. The CPDMF mimics the general behaviour of the CPDLF: it shows a linear part at high masses ($\log M_c > 2.5$), a broad maximum between $\log M_c = 1.5$ and 2.5, and a slow decline towards lower masses. In spite of the present-day observations only allowing for a comparison of the CPDMF data of extragalactic open clusters drawn from model mass-luminosity relations, the agreement with published values is impressive. We find that for $\log M_c > 2.5$ the CPDMF can by fitted with high confidence by a power law with a slope $\chi = 1.01 \pm 0.04$. We regard the observed coincidence of cluster mass function parameters derived for the Galactic and extragalactic clusters with different methods as indirect evidence that both methods of estimating cluster masses are calibrated consistently and give correct and reliable results.

Inspection of cluster samples with different upper limits for age indicates that cluster mass spectra change with time. At every age the cluster mass function keeps the basic features of the CPDMF, i.e., a quasi-linear high-mass portion, and a nonlinear portion at lower masses. With time, the slope of the linear portion increases from $\chi = 0.66 \pm 0.14$ at $\log t \leq 6.9$

to $\chi = 1.13 \pm 0.08$ at $\log t \leq 8.5$. Then the steepening of the CPDMF slows down and arrives at $\chi = 1.17 \pm 0.07$ for $\log t \leq 9.5$. The low-mass portion changes from an approximately flat distribution at $\log t = 6.9$ to a clearly non-linear behaviour displaying a broad maximum with a peak at about 100 $M_\odot$.

We construct the CIMF from the data of a subsample of the 49 youngest clusters with $\log t \leq 6.9$. The CIMF has a segmented structure with two power-law segments: the power-law slopes are $\alpha = 1.66 \pm 0.14$ for $\log M_c = 3.37 \ldots 4.93$ and $\alpha = 0.82 \pm 0.14$ for $\log M_c = 1.7 \ldots 3.37$.

The luminosity function of open clusters does not show the same systematic steepening with age as does the mass function. It evolves via parallel-shifting along the ordinate without changing the slope. Only the faintest segment of the CLF seems to depend on age and spreads towards the fainter magnitudes with age. The weak dependence on age and the presence of a mixture of clusters with different masses in every magnitude bin makes it difficult to determine the CIMF from the CLF.

When comparing the average mass of the newly formed, youngest clusters $\overline{M}_c^{\rm CIMF} \simeq 4.5 \times 10^3\, M_\odot$ with the average cluster mass from the whole sample ($\overline{M}_c^{\rm CPDMF} \simeq 700\, M_\odot$), one finds, as expected, that clusters are typically much more massive at birth than later. Since this observation concerns "normal" optical clusters, one should acknowledge the importance of a continuous mass loss occurring in open clusters during their evolution with a rate around $3{-}14\, M_\odot\,{\rm Myr}^{-1}$.

If this effect is not taken into account, one underestimates the role that open clusters play in supplying the Galactic disc with the products of their evolution: stars and stellar remnants, substellar objects, gas and dust. Provided that the cluster formation history has not changed dramatically in the solar neighbourhood during the evolution of the Galactic disc, at least 40% of the observed surface density of the disc comes from open clusters. The other half is left for violent events (strong winds, HII zones, or supernova explosions) provoking the fast mass loss during the "infant" phase of cluster evolution proposed first by Tutukov (1978) and later by Kroupa et al. (2001), and recently considered in detail by Baumgardt & Kroupa (2007) and Weidner et al. (2007).

Acknowledgements. We thank the anonymous referee for his/her useful comments. This study was supported by DFG grant 436 RUS 113/757/0-2, and RFBR grants 06-02-16379, 07-02-91566.

References

Battinelli, P., & Capuzzo-Dolcetta, R. 1991, MNRAS, 249, 76
Baumgardt, H., & Kroupa, P. 2007, MNRAS, 380, 1589
Baumgardt, H., & Makino, J. 2003, MNRAS, 340, 227
de Grijs, R., Anders, P., Bastian, N., et al. 2003, MNRAS, 343, 1285
Elmegreen, B. G., & Clemens, C. 1985, ApJ, 294, 523
Gieles, M., Larsen, S. S., Bastian, N., & Stein, I. T. 2006, A&A, 450, 129
Holmberg, J., & Flynn, C. 2004, MNRAS, 352, 440
Kharchenko, N. V. 2001, Kinem. Phys. Celest. Bodies, 17, 409
Kharchenko, N. V., Piskunov, A. E., Röser, S., Schilbach, E., & Scholz, R.-D. 2004, Astron. Nachr., 325, 743
Kharchenko, N. V., Piskunov, A. E., Röser, S., Schilbach, E., & Scholz, R.-D. 2005a, A&A, 438, 1163
Kharchenko, N. V., Piskunov, A. E., Röser, S., Schilbach, E., & Scholz, R.-D. 2005b, A&A, 440, 403
Kharchenko, N. V., Scholz, R.-D., Piskunov, A., & Röser, S. E. S. 2007, AN, 328, 889
Kroupa, P. 1995, MNRAS, 277, 1491
Kroupa, P., & Boily, C. M. 2002, MNRAS, 336, 1188
Kroupa, P., Aarseth, S., & Hurley, J. 2001, MNRAS, 321, 699
Lada, C. J., & Lada, E. A. 2003, ARA&A, 41, 57
Lada, E. A., Bally, J., & Stark, A. A. 1991, ApJ, 368, 432
Lamers, H. J. G. L. M., Gieles, M., Bastian, N., et al. 2005, A&A, 441, 117
Larsen, S. S. 2002, AJ, 124, 1393
Megeath, S. T., Flaherty, K. M., Hora, J., et al. 2005, in Massive star birth: A crossroads of Astrophysics, ed. R. Cesaroni, M. Felli, E. Churchwell, & M. Walmsley, IAU Symp. Proc., 227 (Cambridge: Cambridge University Press), 383
Miller, G. E., & Scalo, J. M. 1978, PASP, 90, 506
Parmentier, G., Goodwin, S. P., Kroupa, P., & Baumgardt, H. 2008, ApJ, 678, 347
Piskunov, A. E., Kharchenko, N. V., Röser, S., Schilbach, E., & Scholz, R.-D. 2006, A&A, 445, 545
Piskunov, A. E., Schilbach, E., Kharchenko, N. V., Röser, S., & Scholz, R.-D. 2007, A&A, 468, 151
Piskunov, A. E., Schilbach, E., Kharchenko, N. V., Röser, S., & Scholz, R.-D. 2008, A&A, 477, 165
Sagar, R., Joshi, U. C., & Sinvhal, S. D. 1983, Bull. Astron. Soc. India, 44, 44
Salpeter, E. E. 1955, ApJ, 121, 161
Schilbach, E., Kharchenko, N. V., Piskunov, A. E., Röser, S., & Scholz, R.-D. 2006, A&A, 456, 523
Tutukov, A. V. 1978, A&A, 70, 57
van den Bergh, S., & Lafontaine, A. 1984, AJ, 89, 1822
Weidner, C., Kroupa, P., Nürnberger, D. E. A., & Sterzik, M. F. 2007, MNRAS, 376, 1879
Wielen, R. 1971, A&A, 13, 309
Zhang, Q., & Fall, S. M. 1999, ApJ, 527, L81
Zinnecker, H., McCaughrean, M. J., & Wilking, B. A. 1993, Protostars and Planets III, 429